Albedo Reconstruction of the Apollo Metric Camera Zone.

Ara V Nefian[1,2], Oleg Alexandrov[1], Taemin Kim[2], Zack Moratto[1], and Ross Beyer[3], [1]Carnegie Mellon University, [2]NASA Ames Research Center, MS 245-3, Moffett Field, CA, USA (ara.nefian@nasa.gov),[3]Carl Sagan Center at the SETI Institute

Recently scanned images of the Apollo Metric Camera flown onboard the Apollo 15, 16 and 17 missions contain rich information, including the exposure time and the sun and camera position at the time of image capture. These images, the newly released digital terrain models of the Apollo Metric zone, and accurate photometric models are used to reconstruct at full resolution (10 meters/pixel) the Lunar albedo of the Apollo zone and cover approximately 16% of the Lunar surface. For comparison, the LRO-WAC albedo mosaic covers 100% of the Lunar surface at 100 meters/pixel and the current LRO-NAC derived albedo mosaic covers about 2% of the Lunar surface at 1 meter/pixel resolution.

Introduction

The Apollo Metric camera (AMC) images are scanned at an approximate resolution of 20,000$\times$ 20,000 pixels and have an average overlap of 75$\%$ between consecutive images. Compared to imagery obtained from more recent missions, the images captured on film by the Apollo missions have more noise artifacts, as well as errors in exposure time and camera position and orientation, making the processing of this data significantly more challenging. The stereo pairs are used to generate high resolution digital terrain models (DTM) using the Ames Stereo Pipeline [1]. A robust bundle adjustment technique [2] refines the original estimates for the orientation and position of the AMC.

Image Formation, Modeling and Reconstruction

Let $I_{ij}^k, A_{ij}, X_{ij}, R_{ij}^k, T^k$ be the observed image value, albedo, DTM, reflectance, and exposure time at pixel ij and k-th image. Consider the cost function

$$\mathbf{Q} = \sum_k \sum_{ij} \left[(I_{ij}^k - A_{ij} T^k R_{ij}^k)^2 S_{ij}^k w_{ij}^k \right] \quad (1)$$

In the above equation, the reflectance R_{ij}^k is computed using the Lunar-Lambertian model and is given by

$$R_{ij}^k = (e^{-c_1 \alpha} + c_2) \left[(1 - L(\alpha)) \cos(\mathbf{i}_{ij}^k) + 2L(\alpha) \frac{\cos(\mathbf{i}_{ij}^k)}{\cos(\mathbf{i}_{ij}^k) + \cos(\mathbf{e}_{ij}^k)} \right] \quad (2)$$

where $L(\alpha)$ is a weighting factor between the Lunar and Lambertian reflectance models [3] that depends on the phase angle and surface properties. The quantities α_{ij}^k, $\mathbf{i}_{ij}^k$ and $\mathbf{e}_{ij}^k$ are the phase, incidence and emission angles at pixel ij in k-th DTM respectively. The overall albedo reconstruction system is shown in Figure 1. The

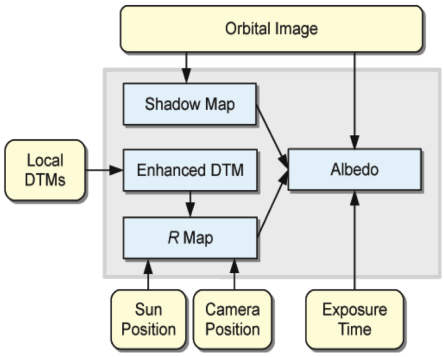

Figure 1: The albedo reconstruction overall system.

system starts with the removal of shadow areas where the terrain models are unreliable and photometric reconstruction is inaccurate. A weighted average of the stereo-derived DTM values determines the DTM values used in computing the local slopes and reflectance. The weights are between 0 and 1. They decrease linearly from the center of the image to the edges. Finally, the albedo is reconstructed by joint estimation of the set $\{c_1, c_2, \tilde{A}_{ij}, \tilde{T}^k\} = \arg\min_{c_1, c_2, A_{ij}, T^k} \mathbf{Q}$. An iterative solution to the above least square problem is given by the Gauss-Newton method. The reconstructed albedo is shown in Figure 2 on top of the Clementine mission mosaic. It is important to note the almost seamless transition between the Apollo reconstructed albedo and the Clementine image mosaic. Together with the albedo mosaic we released the confidence map consisting of albedo reconstructed error (Figure 2 bottom) associated with each pixel of the albedo mosaic and given by:

$$E_{ij} = \frac{\sum_k (I_{ij}^k / (T^k R_{ij}^k) - A_{ij})^2 S_{ij}^k w_{ij}^k}{\sum_k w_{ij}^k} \quad (3)$$

Figure 3 presents in more detail differences between the image mosaic (top) and the reconstructed albedo mosaic (bottom). It can be seen by comparison that the reconstructed albedo significantly reduces most of the brightness artifacts of overlapping images. Figure 4 shows the effect of shadow removal and albedo reconstruction in shadowed areas (right). Figure 5 shows the original im-

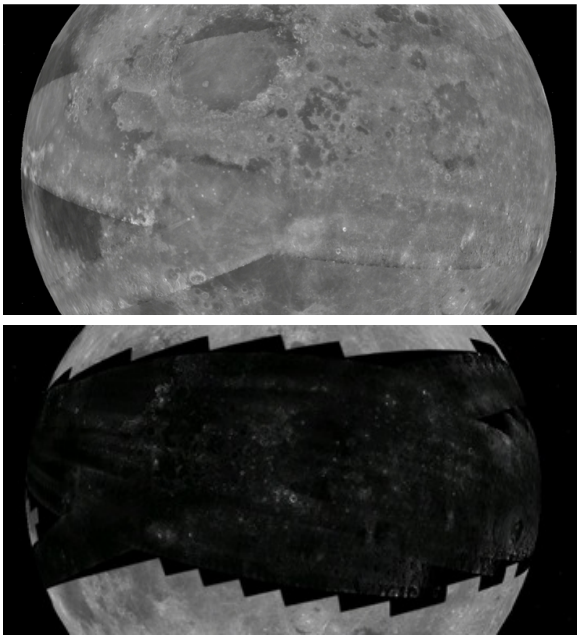

Figure 2: Albedo reconstruction (top) and reconstruction error (bottom) for the Apollo Metric zone.

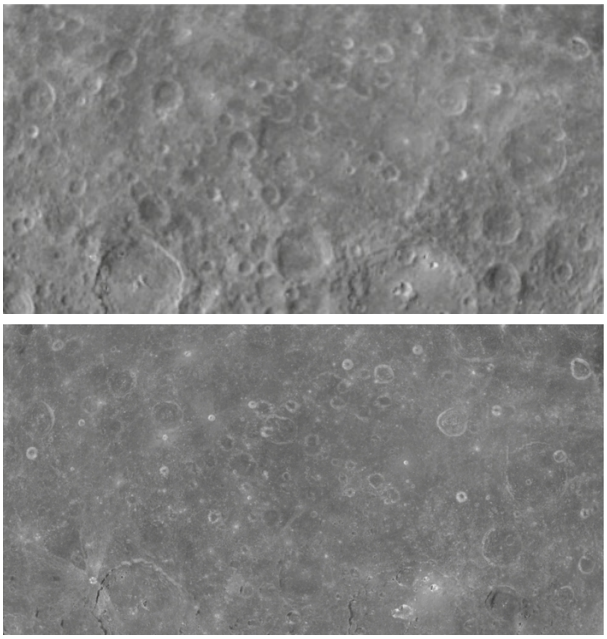

Figure 3: Image mosaic detail (top) and reconstructed albedo (bottom).

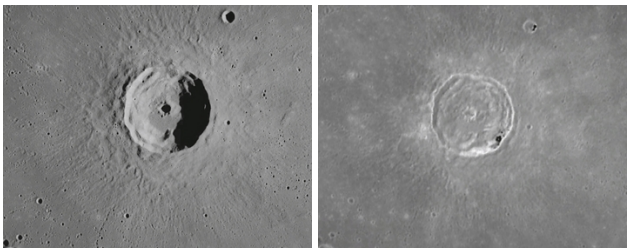

Figure 4: Image mosaic detail (left) and reconstructed albedo with shadow removal (right).

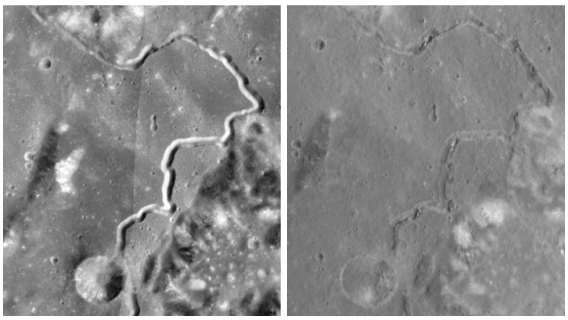

Figure 5: Image mosaic detail (left) and reconstructed albedo (right) for the Apollo 15 landing site.

age mosaic (left) and the reconstructed albedo over the Hadley Rille area.

References

[1] A. Nefian, K. Husmann, M. Broxton, V. To, M. Lundy, and M. Hancher. A Bayesian formulation for sub-pixel refinement in stereo orbital imagery. *International Conference on Image Processing*, 2009.

[2] M. J. Broxton, A. V. Nefian, Z. Moratto, T. Kim, M. Lundy, and A. V. Segal. 3D lunar terrain reconstruction from Apollo images. *International Symposium on Visual Computing*, 2009.

[3] R. W. Gaskell, O. S. Barnouin-Jha, D. J. Scheeres, A. S. Konopliv, T. Mukai, S. Abe, J. Saito, M. Ishiguro, T. Kubota, T. Hashimoto, J. Kawaguchi, M. Yoshikawa, K. Shirakawa, T. Kominato, N. Hirata, and H. Demura. Characterizing and navigating small bodies with imaging data. *Meteoritics and Planetary Science*, 43:1049–1061, September 2008.